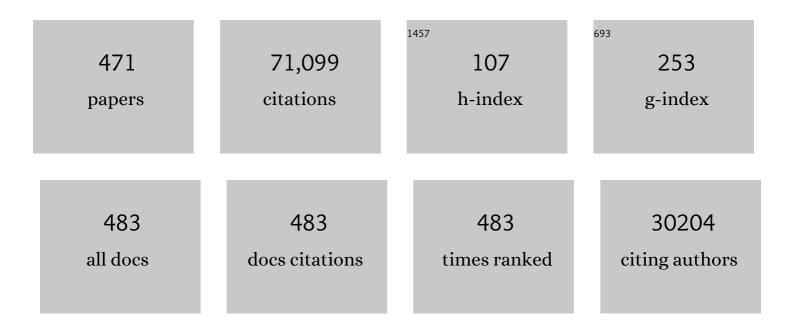
R Lawrence Edwards

List of Publications by Year in descending order

Source: https://exaly.com/author-pdf/5759015/publications.pdf Version: 2024-02-01



#	Article	IF	CITATIONS
1	IntCal13 and Marine13 Radiocarbon Age Calibration Curves 0–50,000 Years cal BP. Radiocarbon, 2013, 55, 1869-1887.	0.8	9,487
2	IntCal09 and Marine09 Radiocarbon Age Calibration Curves, 0–50,000 Years cal BP. Radiocarbon, 2009, 51, 1111-1150.	0.8	4,009
3	The IntCal20 Northern Hemisphere Radiocarbon Age Calibration Curve (0–55 cal kBP). Radiocarbon, 2020, 62, 725-757.	0.8	3,502
4	Intcal04 Terrestrial Radiocarbon Age Calibration, 0–26 Cal Kyr BP. Radiocarbon, 2004, 46, 1029-1058.	0.8	3,238
5	A High-Resolution Absolute-Dated Late Pleistocene Monsoon Record from Hulu Cave, China. Science, 2001, 294, 2345-2348.	6.0	2,594
6	The Holocene Asian Monsoon: Links to Solar Changes and North Atlantic Climate. Science, 2005, 308, 854-857.	6.0	2,115
7	Millennial- and orbital-scale changes in the East Asian monsoon over the past 224,000 years. Nature, 2008, 451, 1090-1093.	13.7	1,567
8	A high-resolution, absolute-dated Holocene and deglacial Asian monsoon record from Dongge Cave, China. Earth and Planetary Science Letters, 2005, 233, 71-86.	1.8	1,510
9	The half-lives of uranium-234 and thorium-230. Chemical Geology, 2000, 169, 17-33.	1.4	1,072
10	238U234U230Th232Th systematics and the precise measurement of time over the past 500,000 years. Earth and Planetary Science Letters, 1987, 81, 175-192.	1.8	1,068
11	Marine04 Marine Radiocarbon Age Calibration, 0–26 Cal Kyr Bp. Radiocarbon, 2004, 46, 1059-1086.	0.8	1,040
12	Timing, Duration, and Transitions of the Last Interglacial Asian Monsoon. Science, 2004, 304, 575-578.	6.0	1,013
13	Improvements in 230Th dating, 230Th and 234U half-life values, and U–Th isotopic measurements by multi-collector inductively coupled plasma mass spectrometry. Earth and Planetary Science Letters, 2013, 371-372, 82-91.	1.8	1,007
14	The Asian monsoon over the past 640,000 years and ice age terminations. Nature, 2016, 534, 640-646.	13.7	956
15	A Test of Climate, Sun, and Culture Relationships from an 1810-Year Chinese Cave Record. Science, 2008, 322, 940-942.	6.0	873
16	238U,234U and232Th in seawater. Earth and Planetary Science Letters, 1986, 80, 241-251.	1.8	844
17	El Niño/Southern Oscillation and tropical Pacific climate during the last millennium. Nature, 2003, 424, 271-276.	13.7	797

18 Ice Age Terminations. Science, 2009, 326, 248-252.

6.0 794

#	Article	IF	CITATIONS
19	The Last Glacial Termination. Science, 2010, 328, 1652-1656.	6.0	702
20	Wet periods in northeastern Brazil over the past 210 kyr linked to distant climate anomalies. Nature, 2004, 432, 740-743.	13.7	698
21	Sea-Surface Temperature from Coral Skeletal Strontium/Calcium Ratios. Science, 1992, 257, 644-647.	6.0	677
22	A Large Drop in Atmospheric 14C/12C and Reduced Melting in the Younger Dryas, Documented with 230Th Ages of Corals. Science, 1993, 260, 962-968.	6.0	470
23	Chinese cave records and the East Asia Summer Monsoon. Quaternary Science Reviews, 2014, 83, 115-128.	1.4	452
24	Climate change patterns in Amazonia and biodiversity. Nature Communications, 2013, 4, 1411.	5.8	422
25	Rapid sea-level fall and deep-ocean temperature change since the last interglacial period. Earth and Planetary Science Letters, 2003, 206, 253-271.	1.8	417
26	Uranium and thorium isotopic and concentration measurements by magnetic sector inductively coupled plasma mass spectrometry. Chemical Geology, 2002, 185, 165-178.	1.4	395
27	Timing and climatic impact of Greenland interstadials recorded in stalagmites from northern Turkey. Geophysical Research Letters, 2009, 36, .	1.5	379
28	Highly Variable El Niño–Southern Oscillation Throughout the Holocene. Science, 2013, 339, 67-70.	6.0	373
29	The variation of summer monsoon precipitation in central China since the last deglaciation. Earth and Planetary Science Letters, 2010, 291, 21-31.	1.8	355
30	The earliest unequivocally modern humans in southern China. Nature, 2015, 526, 696-699.	13.7	354
31	The climatic cyclicity in semiaridâ€arid central Asia over the past 500,000 years. Geophysical Research Letters, 2012, 39, .	1.5	348
32	The Timing of High Sea Levels Over the Past 200,000 Years. Science, 1994, 263, 796-800.	6.0	340
33	Extremely Large Variations of Atmospheric 14C Concentration During the Last Glacial Period. Science, 2001, 292, 2453-2458.	6.0	334
34	Precise Timing of the Last Interglacial Period from Mass Spectrometric Determination of Thorium-230 in Corals. Science, 1987, 236, 1547-1553.	6.0	333
35	Early human occupation of the Red Sea coast of Eritrea during the last interglacial. Nature, 2000, 405, 65-69.	13.7	327
36	Sea-level variability over five glacial cycles. Nature Communications, 2014, 5, 5076.	5.8	325

#	Article	IF	CITATIONS
37	Earthquake Supercycles Inferred from Sea-Level Changes Recorded in the Corals of West Sumatra. Science, 2008, 322, 1674-1678.	6.0	323
38	The Global Paleomonsoon as seen through speleothem records from Asia and the Americas. Climate Dynamics, 2012, 39, 1045-1062.	1.7	311
39	800,000 Years of Abrupt Climate Variability. Science, 2011, 334, 347-351.	6.0	310
40	Climate and Vegetation History of the Midcontinent from 75 to 25 ka: A Speleothem Record from Crevice Cave, Missouri, USA. , 1998, 282, 1871-1874.		292
41	High-precision and high-resolution carbonate 230Th dating by MC-ICP-MS with SEM protocols. Geochimica Et Cosmochimica Acta, 2012, 99, 71-86.	1.6	277
42	Onset of deglacial warming in West Antarctica driven by local orbital forcing. Nature, 2013, 500, 440-444.	13.7	276
43	Orbitally driven east–west antiphasing of SouthÂAmerican precipitation. Nature Geoscience, 2009, 2, 210-214.	5.4	275
44	Hydroclimate changes across the Amazon lowlands over the past 45,000 years. Nature, 2017, 541, 204-207.	13.7	263
45	The GEOTRACES Intermediate Data Product 2017. Chemical Geology, 2018, 493, 210-223.	1.4	257
46	Timing and structure of the 8.2 kyr B.P. event inferred from δ18O records of stalagmites from China, Oman, and Brazil. Geology, 2009, 37, 1007-1010.	2.0	251
47	Abrupt changes in early Holocene tropical sea surface temperature derived from coral records. Nature, 1997, 385, 705-707.	13.7	250
48	Variability of Southwest Indian summer monsoon precipitation during the BÃ,lling-ÃllerÃ,d. Geology, 2005, 33, 813.	2.0	243
49	Interhemispheric anti-phasing of rainfall during the last glacial period. Quaternary Science Reviews, 2006, 25, 3391-3403.	1.4	242
50	A high-resolution stalagmite record of the Holocene East Asian monsoon from Mt Shennongjia, central China. Holocene, 2010, 20, 257-264.	0.9	242
51	A 900â€year (600 to 1500 A.D.) record of the Indian summer monsoon precipitation from the core monsoon zone of India. Geophysical Research Letters, 2007, 34, .	1.5	239
52	Millennialâ€scale precipitation changes in southern Brazil over the past 90,000 years. Geophysical Research Letters, 2007, 34, .	1.5	237
53	Variability of stalagmite-inferred Indian monsoon precipitation over the past 252,000 y. Proceedings of the National Academy of Sciences of the United States of America, 2015, 112, 2954-2959.	3.3	233
54	A penultimate glacial monsoon record from Hulu Cave and two-phase glacial terminations. Geology, 2006, 34, 217.	2.0	232

#	Article	IF	CITATIONS
55	Annual growth banding in a cave stalagmite. Nature, 1993, 364, 518-520.	13.7	231
56	Deep-Sea Coral Evidence for Rapid Change in Ventilation of the Deep North Atlantic 15,400 Years Ago. Science, 1998, 280, 725-728.	6.0	227
57	Actively evolving microplate formation by oblique collision and sideways motion along strike-slip faults: An example from the northeastern Caribbean plate margin. Tectonophysics, 1995, 246, 1-69.	0.9	226
58	Human remains from Zhirendong, South China, and modern human emergence in East Asia. Proceedings of the National Academy of Sciences of the United States of America, 2010, 107, 19201-19206.	3.3	223
59	Stable isotope variations in modern tropical speleothems: Evaluating equilibrium vs. kinetic isotope effects. Geochimica Et Cosmochimica Acta, 2004, 68, 4381-4393.	1.6	218
60	Putting the Younger Dryas cold event into context. Quaternary Science Reviews, 2010, 29, 1078-1081.	1.4	218
61	Early Neanderthal constructions deep in Bruniquel Cave in southwestern France. Nature, 2016, 534, 111-114.	13.7	210
62	U-Th dating of deep-sea corals. Geochimica Et Cosmochimica Acta, 2000, 64, 2401-2416.	1.6	205
63	Direct Determination of the Timing of Sea Level Change During Termination II. Science, 2002, 295, 310-313.	6.0	204
64	Abrupt changes in Indian summer monsoon strength during 33,800 to 5500 years B.P Geophysical Research Letters, 2015, 42, 5526-5532.	1.5	198
65	High-Latitude Forcing of the South American Summer Monsoon During the Last Glacial. Science, 2012, 335, 570-573.	6.0	196
66	Indian monsoon variability on millennial-orbital timescales. Scientific Reports, 2016, 6, 24374.	1.6	194
67	A +20 m middle Pleistocene sea-level highstand (Bermuda and the Bahamas) due to partial collapse of Antarctic ice. Geology, 1999, 27, 375.	2.0	189
68	The Indian monsoon variability and civilization changes in the Indian subcontinent. Science Advances, 2017, 3, e1701296.	4.7	188
69	Protactinium-231 Dating of Carbonates by Thermal Ionization Mass Spectrometry: Implications for Quaternary Climate Change. Science, 1997, 276, 782-786.	6.0	184
70	North Atlantic storm track changes during the Last Glacial Maximum recorded by Alpine speleothems. Nature Communications, 2015, 6, 6344.	5.8	183
71	Archaea and bacteria with surprising microdiversity show shifts in dominance over 1,000-year time scales in hydrothermal chimneys. Proceedings of the National Academy of Sciences of the United States of America, 2010, 107, 1612-1617.	3.3	181
72	Climate on the southern Black Sea coast during the Holocene: implications from the Sofular Cave record. Quaternary Science Reviews, 2011, 30, 2433-2445.	1.4	181

#	Article	IF	CITATIONS
73	Submergence and uplift associated with the giant 1833 Sumatran subduction earthquake: Evidence from coral microatolls. Journal of Geophysical Research, 1999, 104, 895-919.	3.3	177
74	Pleistocene water intrusions from the Mediterranean and Caspian seas into theÂBlackÂSea. Nature Geoscience, 2011, 4, 236-239.	5.4	177
75	Trends and oscillations in the Indian summer monsoon rainfall over the last two millennia. Nature Communications, 2015, 6, 6309.	5.8	177
76	Annual cycles of in coral skeletons and thermometry. Geochimica Et Cosmochimica Acta, 1995, 59, 2025-2042.	1.6	176
77	Source parameters of the great Sumatran megathrust earthquakes of 1797 and 1833 inferred from coral microatolls. Journal of Geophysical Research, 2006, 111, n/a-n/a.	3.3	176
78	A global context for megadroughts in monsoon Asia during the past millennium. Quaternary Science Reviews, 2011, 30, 47-62.	1.4	176
79	The WAIS Divide deep ice core WD2014 chronology – Part 1: Methane synchronization (68–31 ka BP) and the gas age–ice age difference. Climate of the Past, 2015, 11, 153-173.	1.3	172
80	The Holocene Indian monsoon variability over the southern Tibetan Plateau and its teleconnections. Earth and Planetary Science Letters, 2012, 335-336, 135-144.	1.8	171
81	Measurement of Attogram Quantities of231Pa in Dissolved and Particulate Fractions of Seawater by Isotope Dilution Thermal Ionization Mass Spectroscopy. Analytical Chemistry, 2003, 75, 1075-1079.	3.2	168
82	Variation of initial 230Th/232Th and limits of high precision U–Th dating of shallow-water corals. Geochimica Et Cosmochimica Acta, 2008, 72, 4201-4223.	1.6	162
83	A speleothem record of glacial (25–11.6 kyr BP) rapid climatic changes from northern Iberian Peninsula. Global and Planetary Change, 2010, 71, 218-231.	1.6	152
84	High resolution characterization of the Asian Monsoon between 146,000 and 99,000Âyears B.P. from Dongge Cave, China and global correlation of events surrounding Termination II. Palaeogeography, Palaeoclimatology, Palaeoecology, 2006, 236, 20-38.	1.0	146
85	Persistent multidecadal power of the Indian Summer Monsoon. Earth and Planetary Science Letters, 2010, 290, 166-172.	1.8	144
86	Authigenic carbonates from seeps on the northern continental slope of the South China Sea: New insights into fluid sources and geochronology. Marine and Petroleum Geology, 2013, 43, 260-271.	1.5	143
87	The climate variability in northern Levant over the past 20,000 years. Geophysical Research Letters, 2015, 42, 8641-8650.	1.5	142
88	U-series dating and taphonomy of Quaternary vertebrates from Brazilian caves. Palaeogeography, Palaeoclimatology, Palaeoecology, 2006, 240, 508-522.	1.0	139
89	Uranium-series Dating of Marine and Lacustrine Carbonates. Reviews in Mineralogy and Geochemistry, 2003, 52, 363-405.	2.2	137
90	A high-resolution record of atmospheric 14C based on Hulu Cave speleothem H82. Quaternary Science Reviews, 2012, 33, 32-41.	1.4	136

#	Article	IF	CITATIONS
91	Climate variations of Central Asia on orbital to millennial timescales. Scientific Reports, 2016, 6, 36975.	1.6	136
92	Quaternary ecological and geomorphic changes associated with rainfall events in presently semi-arid northeastern Brazil. Journal of Quaternary Science, 2004, 19, 693-701.	1.1	134
93	Selection and Treatment of Data for Radiocarbon Calibration: An Update to the International Calibration (IntCal) Criteria. Radiocarbon, 2013, 55, 1923-1945.	0.8	134
94	Stalagmite evidence from Belize indicating significant droughts at the time of Preclassic Abandonment, the Maya Hiatus, and the Classic Maya collapse. Palaeogeography, Palaeoclimatology, Palaeoecology, 2007, 250, 1-17.	1.0	130
95	Paleoclimate reconstruction in the Levant region from the geochemistry of a Holocene stalagmite from the Jeita cave, Lebanon. Quaternary Research, 2008, 70, 368-381.	1.0	128
96	NALPS: a precisely dated European climate record 120â \in 60 ka. Climate of the Past, 2011, 7, 1247-1259.	1.3	127
97	High-resolution absolute-dated Indian Monsoon record between 53 and 36 ka from Xiaobailong Cave, southwestern China. Geology, 2006, 34, 621.	2.0	125
98	High-resolution variability of the South American summer monsoon over the last seven millennia: insights from a speleothem record from the central Peruvian Andes. Quaternary Science Reviews, 2013, 75, 1-10.	1.4	124
99	Holocene moisture changes in western China, Central Asia, inferred from stalagmites. Quaternary Science Reviews, 2017, 158, 15-28.	1.4	124
100	Long-term trend and abrupt events of the Holocene Asian monsoon inferred from a stalagmite δ100 record from Shennongjia in Central China. Science Bulletin, 2006, 51, 221-228.	1.7	123
101	Land surface temperature changes in Northern Iberia since 4000yrBP, based on δ13C of speleothems. Global and Planetary Change, 2011, 77, 1-12.	1.6	122
102	Potential role of winter rainfall in explaining increased moisture in the Mediterranean and Middle East during periods of maximum orbitally-forced insolation seasonality. Climate Dynamics, 2014, 42, 1079-1095.	1.7	122
103	Timing and structure of the Younger Dryas event and its underlying climate dynamics. Proceedings of the United States of America, 2020, 117, 23408-23417.	3.3	119
104	Quaternary glaciation and hydrologic variation in the South American tropics as reconstructed from the Lake Titicaca drilling project. Quaternary Research, 2007, 68, 410-420.	1.0	117
105	A high-resolution history of the South American Monsoon from Last Glacial Maximum to the Holocene. Scientific Reports, 2017, 7, 44267.	1.6	117
106	Abrupt variations in South American monsoon rainfall during the Holocene based on a speleothem record from central-eastern Brazil. Geology, 2011, 39, 1075-1078.	2.0	116
107	Coupling of Indo-Pacific climate variability over the last millennium. Nature, 2020, 579, 385-392.	13.7	116
108	Maximum sea levels for the last glacial period from U-series ages of submerged speleothems. Nature, 1994, 367, 357-360.	13.7	110

#	Article	IF	CITATIONS
109	Sequence of mammalian fossils, including hominoid teeth, from the Bubing Basin caves, South China. Journal of Human Evolution, 2007, 52, 370-379.	1.3	109
110	U/Th-dating living and young fossil corals from the central tropical Pacific. Earth and Planetary Science Letters, 2003, 210, 91-103.	1.8	107
111	Summer monsoon precipitation variations in central China over the past 750years derived from a high-resolution absolute-dated stalagmite. Palaeogeography, Palaeoclimatology, Palaeoecology, 2009, 280, 432-439.	1.0	106
112	Dating earthquakes with high-precision thorium-230 ages of very young corals. Earth and Planetary Science Letters, 1988, 90, 371-381.	1.8	102
113	Paleogeodetic records of seismic and aseismic subduction from central Sumatran microatolls, Indonesia. Journal of Geophysical Research, 2004, 109, .	3.3	101
114	High-resolution Holocene South American monsoon history recorded by a speleothem from BotuverÃi Cave, Brazil. Earth and Planetary Science Letters, 2016, 450, 186-196.	1.8	101
115	Timing and structure of the Younger Dryas event in northern China. Quaternary Science Reviews, 2012, 41, 83-93.	1.4	96
116	Multidecadal climate variability in Brazil's Nordeste during the last 3000 years based on speleothem isotope records. Geophysical Research Letters, 2012, 39, .	1.5	96
117	Timing and structure of Megaâ€SACZ events during Heinrich Stadial 1. Geophysical Research Letters, 2015, 42, 5477.	1.5	93
118	Centennial- to decadal-scale monsoon precipitation variations in the upper Hanjiang River region, China over the past 6650 years. Earth and Planetary Science Letters, 2018, 482, 580-590.	1.8	93
119	High resolution monsoon precipitation changes on southeastern Tibetan Plateau over the past 2300 years. Quaternary Science Reviews, 2018, 195, 122-132.	1.4	93
120	Seasonal and interannual variability of the Mid-Holocene East Asian monsoon in coral δ180 records from the South China Sea. Earth and Planetary Science Letters, 2005, 237, 69-84.	1.8	91
121	Accelerated drawdown of meridional overturning in the late-glacial Atlantic triggered by transient pre-H event freshwater perturbation. Geophysical Research Letters, 2006, 33, .	1.5	89
122	Geochronology of late Pleistocene to Holocene speleothemsfrom central Texas: Implications for regional paleoclimate. Bulletin of the Geological Society of America, 2001, 113, 1532-1543.	1.6	87
123	Atmospheric ¹⁴ C/ ¹² C changes during the last glacial period from Hulu Cave. Science, 2018, 362, 1293-1297.	6.0	86
124	Time-scales of Differentiation from Mafic Parents to Rhyolite in North American Continental Arcs. Journal of Petrology, 2003, 44, 1703-1726.	1.1	85
125	Enhanced El Niño–Southern Oscillation Variability in Recent Decades. Geophysical Research Letters, 2020, 47, e2019GL083906.	1.5	85
126	South American monsoon response to iceberg discharge in the North Atlantic. Proceedings of the National Academy of Sciences of the United States of America, 2018, 115, 3788-3793.	3.3	84

#	Article	IF	CITATIONS
127	Dissolved and particulate 231 Pa and 230 Th in the Atlantic Ocean: constraints on intermediate/deep water age, boundary scavenging, and 231 Pa/ 230 Th fractionation. Earth and Planetary Science Letters, 2002, 203, 999-1014.	1.8	83
128	Uranium-series coral ages from the US Atlantic Coastal Plain–the "80ka problem―revisited. Quaternary International, 2004, 120, 3-14.	0.7	83
129	A new perspective on the hydroclimate variability in northern South America during the Little Ice Age. Geophysical Research Letters, 2009, 36, .	1.5	83
130	Intensity of Th and Pa scavenging partitioned by particle chemistry in the North Atlantic Ocean. Marine Chemistry, 2015, 170, 49-60.	0.9	83
131	Uranium-thorium-protactinium dating systematics. Geochimica Et Cosmochimica Acta, 1998, 62, 3437-3452.	1.6	82
132	Speleothem climate records from deep time? Exploring the potential with an example from the Permian. Geology, 2010, 38, 455-458.	2.0	82
133	High-precision U-series dating of Locality 1 at Zhoukoudian, China. Journal of Human Evolution, 2001, 41, 679-688.	1.3	81
134	Central Europe temperature constrained by speleothem fluid inclusion water isotopes over the past 14,000 years. Science Advances, 2019, 5, eaav3809.	4.7	81
135	Collapse of the Liangzhu and other Neolithic cultures in the lower Yangtze region in response to climate change. Science Advances, 2021, 7, eabi9275.	4.7	81
136	The Transpolar Drift as a Source of Riverine and Shelfâ€Derived Trace Elements to the Central Arctic Ocean. Journal of Geophysical Research: Oceans, 2020, 125, e2019JC015920.	1.0	80
137	A High-Resolution Radiocarbon Calibration Between 11,700 and 12,400 Calendar Years Bp Derived from ²³⁰ Th Ages of Corals from Espiritu Santo Island, Vanuatu. Radiocarbon, 1998, 40, 1093-1105.	0.8	79
138	230Th and 231Pa on GEOTRACES GA03, the U.S. GEOTRACES North Atlantic transect, and implications for modern and paleoceanographic chemical fluxes. Deep-Sea Research Part II: Topical Studies in Oceanography, 2015, 116, 29-41.	0.6	79
139	Multi-speleothem record reveals tightly coupled climate between central Europe and Greenland during Marine Isotope Stage 3. Geology, 2014, 42, 1043-1046.	2.0	77
140	High-resolution temporal record of Holocene ground-water chemistry: Tracing links between climate and hydrology. Geology, 1996, 24, 1049.	2.0	76
141	Rapid forearc uplift and subsidence caused by impinging bathymetric features: Examples from the New Hebrides and Solomon arcs. Tectonics, 2005, 24, n/a-n/a.	1.3	75
142	Precipitation evolution of Central Asia during the last 5000 years. Holocene, 2017, 27, 142-154.	0.9	75
143	Distribution of 230Th in the Labrador Sea and its relation to ventilation. Earth and Planetary Science Letters, 1997, 150, 151-160.	1.8	74
144	Large variations of oxygen isotopes in precipitation over south-central Tibet during Marine Isotope Stage 5. Geology, 2010, 38, 243-246.	2.0	73

#	Article	IF	CITATIONS
145	Rainfall variations in central Indo-Pacific over the past 2,700 y. Proceedings of the National Academy of Sciences of the United States of America, 2019, 116, 17201-17206.	3.3	73
146	Decreasing monsoon precipitation in southwest China during the last 240Âyears associated with the warming of tropical ocean. Climate Dynamics, 2017, 48, 1769-1778.	1.7	72
147	A data-model comparison pinpoints Holocene spatiotemporal pattern of East Asian summer monsoon. Quaternary Science Reviews, 2021, 261, 106911.	1.4	72
148	Radiocarbon Calibration and Comparison to 50 Kyr BP with Paired ¹⁴ C and ²³⁰ Th Dating of Corals from Vanuatu and Papua New Guinea. Radiocarbon, 2004, 46, 1127-1160.	0.8	71
149	Abrupt change of Antarctic moisture origin at the end of Termination II. Proceedings of the National Academy of Sciences of the United States of America, 2010, 107, 12091-12094.	3.3	71
150	Centennial-scale solar forcing of the South American Monsoon System recorded in stalagmites. Scientific Reports, 2016, 6, 24762.	1.6	71
151	Early maximum extent of paleoglaciers from Mediterranean mountains during the last glaciation. Scientific Reports, 2013, 3, 2034.	1.6	70
152	U–Th systematics and 230Th ages of carbonate chimneys at the Lost City Hydrothermal Field. Geochimica Et Cosmochimica Acta, 2011, 75, 1869-1888.	1.6	68
153	The Asian Summer Monsoon: Teleconnections and Forcing Mechanisms—A Review from Chinese Speleothem l´180 Records. Quaternary, 2019, 2, 26.	1.0	68
154	No consistent ENSO response to volcanic forcing over the last millennium. Science, 2020, 367, 1477-1481.	6.0	68
155	Mass Spectrometric ¹⁴ C and U-Th Measurements in Coral. Radiocarbon, 1992, 34, 611-618.	0.8	67
156	Continuous reef growth during the last 23calkyr BP in a tectonically active zone (Vanuatu,) Tj ETQq0 0 0 rgBT /C	verlock 10	0 Tf 50 302 To
157	A Speleothem Record of Younger Dryas Cooling, Klamath Mountains, Oregon, USA. Quaternary Research, 2005, 64, 249-256.	1.0	67
158	The Taravilla lake and tufa deposits (Central Iberian Range, Spain) as palaeohydrological and palaeoclimatic indicators. Palaeogeography, Palaeoclimatology, Palaeoecology, 2008, 259, 136-156.	1.0	67
159	Precise dating of abrupt shifts in the Asian Monsoon during the last deglaciation based on stalagmite data from Yamen Cave, Guizhou Province, China. Science China Earth Sciences, 2010, 53, 633-641.	2.3	67
160	Paleoclimate and growth rates of speleothems in the northwestern Iberian Peninsula over the last two glacial cycles. Quaternary Research, 2013, 80, 284-290.	1.0	67
161	Hydroclimate variability of the northwestern Amazon Basin near the Andean foothills of Peru related to the South American Monsoon System during the last 1600 years. Climate of the Past, 2014, 10, 1967-1981.	1.3	67
162	A high-resolved record of the Asian Summer Monsoon from Dongge Cave, China for the past 1200 years. Quaternary Science Reviews, 2015, 122, 250-257.	1.4	67

#	Article	IF	CITATIONS
163	Lake Level Reconstruction for 12.8–2.3 ka of the Ngangla Ring Tso Closed-Basin Lake System, Southwest Tibetan Plateau. Quaternary Research, 2015, 83, 66-79.	1.0	67
164	How well can we quantify dust deposition to the ocean?. Philosophical Transactions Series A, Mathematical, Physical, and Engineering Sciences, 2016, 374, 20150285.	1.6	66
165	Role of climate in the rise and fall of the Neo-Assyrian Empire. Science Advances, 2019, 5, eaax6656.	4.7	66
166	Radiocarbon Dating of Deep-Sea Corals. Radiocarbon, 2002, 44, 567-580.	0.8	65
167	Hydrological change in Southern Europe responding to increasing North Atlantic overturning during Greenland Stadial 1. Proceedings of the National Academy of Sciences of the United States of America, 2015, 112, 6568-6572.	3.3	65
168	Evaluating the timing and structure of the 4.2 ka event in the Indian summer monsoon domain from an annually resolved speleothem record from Northeast India. Climate of the Past, 2018, 14, 1869-1879.	1.3	64
169	The Homo sapiens Cave hominin site of Mulan Mountain, Jiangzhou District, Chongzuo, Guangxi with emphasis on its age. Science Bulletin, 2009, 54, 3848-3856.	1.7	63
170	The timing, two-pulsed nature, and variable climatic expression of the 4.2 ka event: A review and new high-resolution stalagmite data from Namibia. Quaternary Science Reviews, 2018, 186, 78-90.	1.4	63
171	Connecting the Greenland ice-core and Uâ^•Th timescales via cosmogenic radionuclides: testing the synchroneity of Dansgaard–Oeschger events. Climate of the Past, 2018, 14, 1755-1781.	1.3	62
172	Protactinium-231 and Thorium-230 Abundances and High Scavenging Rates in the Western Arctic Ocean. Science, 1998, 280, 405-407.	6.0	61
173	U/Th dating of cold-seep carbonates: An initial comparison. Deep-Sea Research Part II: Topical Studies in Oceanography, 2010, 57, 2055-2060.	0.6	61
174	Lacustrine cave carbonates: Novel archives of paleohydrologic change in the Bonneville Basin (Utah,) Tj ETQq0 0	0 rgBT /Ov	verlock 10 Tf
175	Pressure, Temperature and C-O-H Fluid Fugacities across the Amphibolite-Granulite Transition, Northwest Adirondack Mountains, New York. Journal of Petrology, 1988, 29, 39-72.	1.1	60
176	(231Pa/235U)-(230Th/238U) of young mafic volcanic rocks from Nicaragua and Costa Rica and the influence of flux melting on U-series systematics of arc lavas. Geochimica Et Cosmochimica Acta, 2002, 66, 4287-4309.	1.6	60
177	High-resolution stalagmite l´180 records of Asian monsoon changes in central and southern China spanning the MIS 3/2 transition. Earth and Planetary Science Letters, 2010, 298, 191-198.	1.8	60
178	Cyclic precipitation variation on the western Loess Plateau of China during the past four centuries. Scientific Reports, 2014, 4, 6381.	1.6	60
179	Seismic recurrence intervals and timing of aseismic subduction inferred from emerged corals and reefs of the Central Vanuatu (New Hebrides) Frontal Arc. Journal of Geophysical Research, 1990, 95, 393-408.	3.3	59
180	Petrographic and isotopic evidence for Holocene long-term climate change and shorter-term environmental shifts from a stalagmite from the Serra do Courel of northwestern Spain, and implications for climatic history across Europe and the Mediterranean. Palaeogeography, Palaeoclimatology, Palaeoecology, 2011, 305, 172-184.	1.0	58

#	Article	IF	CITATIONS
181	An evaluation of quantitative reconstruction of past precipitation records using coral skeletal Sr/Ca and δ180 data. Earth and Planetary Science Letters, 2005, 237, 370-386.	1.8	57
182	Termination-II interstadial/stadial climate change recorded in two stalagmites from the north European Alps. Quaternary Science Reviews, 2015, 127, 229-239.	1.4	57
183	Ecosystem and paleohydrological response to Quaternary climate change in the Bonneville Basin, Utah. Palaeogeography, Palaeoclimatology, Palaeoecology, 2005, 221, 99-122.	1.0	56
184	Interseismic deformation above the Sunda Megathrust recorded in coral microatolls of the Mentawai islands, West Sumatra. Journal of Geophysical Research, 2007, 112, .	3.3	56
185	Direct measurements of deglacial monsoon strength in a Chinese stalagmite. Geology, 2015, 43, 555-558.	2.0	56
186	Early-Holocene monsoon instability and climatic optimum recorded by Chinese stalagmites. Holocene, 2019, 29, 1059-1067.	0.9	56
187	Oxygen isotope precipitation anomaly in the North Atlantic region during the 8.2 ka event. Geology, 2009, 37, 1095-1098.	2.0	55
188	Climatic and biotic thresholds of coral-reefÂshutdown. Nature Climate Change, 2015, 5, 369-374.	8.1	55
189	Evidence of a prolonged drought ca. 4200â€⁻yrâ€⁻BP correlated with prehistoric settlement abandonment from the Gueldaman GLD1 Cave, Northern Algeria. Climate of the Past, 2016, 12, 1-14.	1.3	55
190	Variable North Pacific influence on drought in southwestern North America since AD 854. Nature Geoscience, 2013, 6, 617-621.	5.4	54
191	Mid-latitude interhemispheric hydrologic seesaw over the past 550,000 years. Nature, 2014, 508, 378-382.	13.7	54
192	Age of the Laschamp excursion determined by U-Th dating of a speleothem geomagnetic record from North America. Geology, 2016, 44, 139-142.	2.0	54
193	Holocene Monsoon Change and Abrupt Events on the Western Chinese Loess Plateau as Revealed by Accurately Dated Stalagmites. Geophysical Research Letters, 2020, 47, e2020GL090273.	1.5	54
194	Recent Emerged Reef Terraces of the Yenkahe Resurgent Block, Tanna, Vanuatu: Implications for Volcanic, Landslide and Tsunami Hazards. Journal of Geology, 1995, 103, 577-590.	0.7	53
195	87Sr/86Sr and Sr/Ca in speleothems for paleoclimate reconstruction in Central China between 70 and 280 kyr ago. Geochimica Et Cosmochimica Acta, 2005, 69, 3933-3947.	1.6	53
196	GEOTRACES intercalibration of ²³⁰ Th, ²³² Th, ²³¹ Pa, and prospects for ¹⁰ Be. Limnology and Oceanography: Methods, 2012, 10, 179-213.	1.0	53
197	Two Millennia of South Atlantic Convergence Zone Variability Reconstructed From Isotopic Proxies. Geophysical Research Letters, 2018, 45, 5045-5051.	1.5	53
198	A Great Basin-wide dry episode during the first half of the Mystery Interval?. Quaternary Science Reviews, 2009, 28, 2557-2563.	1.4	52

#	Article	IF	CITATIONS
199	Mid- to late Holocene Indian Ocean Monsoon variability recorded in four speleothems from Socotra Island, Yemen. Quaternary Science Reviews, 2013, 65, 129-142.	1.4	52
200	Megadrought and cultural exchange along the proto-silk road. Science Bulletin, 2021, 66, 603-611.	4.3	52
201	Foredeep tectonics and carbonate platform dynamics in the Huon Gulf, Papua New Guinea. Geology, 1996, 24, 819.	2.0	51
202	Speleothem evidence for Holocene fluctuations of the prairie-forest ecotone, north-central USA. Holocene, 1999, 9, 671-676.	0.9	51
203	Cyclic sedimentation in Brazilian caves: Mechanisms and palaeoenvironmental significance. Geomorphology, 2009, 106, 142-153.	1.1	51
204	Panigarh cave stalagmite evidence of climate change in the Indian Central Himalaya since AD 1256: Monsoon breaks and winter southern jet depressions. Quaternary Science Reviews, 2015, 124, 145-161.	1.4	51
205	A detailed comparison of Asian Monsoon intensity and Greenland temperature during the AllerÃ,d and Younger Dryas events. Earth and Planetary Science Letters, 2008, 272, 691-697.	1.8	50
206	Holocene winter climate variability in mid-latitude western North America. Nature Communications, 2012, 3, 1219.	5.8	50
207	The Blake geomagnetic excursion recorded in a radiometrically dated speleothem. Earth and Planetary Science Letters, 2012, 353-354, 173-181.	1.8	50
208	A petrographic and geochemical record of climate change over the last 4600years from a northern Namibia stalagmite, with evidence of abruptly wetter climate at the beginning of southern Africa's Iron Age. Palaeogeography, Palaeoclimatology, Palaeoecology, 2013, 376, 149-162.	1.0	50
209	Speleothems as sensitive recorders of volcanic eruptions – the Bronze Age Minoan eruption recorded in a stalagmite from Turkey. Earth and Planetary Science Letters, 2014, 392, 58-66.	1.8	50
210	Hydroclimatic variations in southeastern China during the 4.2 ka event reflected by stalagmite records. Climate of the Past, 2018, 14, 1805-1817.	1.3	50
211	Ancient DNA and multimethod dating confirm the late arrival of anatomically modern humans in southern China. Proceedings of the National Academy of Sciences of the United States of America, 2021, 118, .	3.3	49
212	Late Quaternary uplift and earthquake potential of the San Joaquin Hills, southern Los Angeles basin, California. Geology, 1999, 27, 1031.	2.0	48
213	Contribution of ENSO variability to the East Asian summer monsoon in the late Holocene. Palaeogeography, Palaeoclimatology, Palaeoecology, 2016, 449, 510-519.	1.0	48
214	A 6000-year high-resolution climatic record from a stalagmite in Xiangshui Cave, Guilin, China. Holocene, 2004, 14, 697-702.	0.9	47
215	U-series isotope evidence for the origin of continental basalts. Earth and Planetary Science Letters, 1995, 134, 1-7.	1.8	46
216	High resolution Secondary Ionisation Mass Spectrometry (SIMS) δ180 analyses of Hulu Cave speleothem at the time of Heinrich Event 1. Chemical Geology, 2007, 238, 197-212.	1.4	46

#	Article	IF	CITATIONS
217	North Atlantic Iceâ€Rafting, Ocean and Atmospheric Circulation During the Holocene: Insights From Western Mediterranean Speleothems. Geophysical Research Letters, 2019, 46, 7614-7623.	1.5	46
218	High precision230Th and232Th in the Norwegian Sea and Denmark by thermal ionization mass spectrometry. Geophysical Research Letters, 1995, 22, 2589-2592.	1.5	45
219	Melting of the Earth's lithospheric mantle inferred from protactinium– thorium–uranium isotopic data. Nature, 2000, 406, 293-296.	13.7	45
220	Stratigraphy and geochronology of pitfall accumulations in caves and fissures, Bermuda. Quaternary Science Reviews, 2004, 23, 1151-1171.	1.4	45
221	Sub-millennial variability of Asian monsoon intensity during the early MIS 3 and its analogue to the ice age terminations. Quaternary Science Reviews, 2010, 29, 1107-1115.	1.4	45
222	A 200-year annually laminated stalagmite record of precipitation seasonality in southeastern China and its linkages to ENSO and PDO. Scientific Reports, 2018, 8, 12344.	1.6	45
223	Pluvial periods in Southern Arabia over the last 1.1 million-years. Quaternary Science Reviews, 2020, 229, 106112.	1.4	45
224	Strong coupling of Asian Monsoon and Antarctic climates on sub-orbital timescales. Scientific Reports, 2016, 6, 32995.	1.6	44
225	Holocene changes in monsoon precipitation in the Andes of NE Peru based on δ180 speleothem records. Quaternary Science Reviews, 2016, 146, 274-287.	1.4	44
226	Reconciliation of the Devils Hole climate record with orbital forcing. Science, 2016, 351, 165-168.	6.0	44
227	The East Asian summer monsoon variability over the last 145 years inferred from the Shihua Cave record, North China. Scientific Reports, 2017, 7, 7078.	1.6	44
228	Historic 1771 Meiwa tsunami confirmed by highâ€resolution U/Th dating of massive <i>Porites</i> coral boulders at Ishigaki Island in the Ryukyus, Japan. Geochemistry, Geophysics, Geosystems, 2010, 11, .	1.0	43
229	The seasonality of east central North American precipitation based on three coeval Holocene speleothems from southern West Virginia. Earth and Planetary Science Letters, 2010, 295, 342-348.	1.8	43
230	Multiple proxy analyses of a U/Th-dated stalagmite to reconstruct paleoenvironmental changes in northwestern Madagascar between 370 CE and 1300 CE. Palaeogeography, Palaeoclimatology, Palaeoecology, 2017, 469, 138-155.	1.0	43
231	Intense hydrothermal scavenging of 230Th and 231Pa in the deep Southeast Pacific. Marine Chemistry, 2018, 201, 212-228.	0.9	42
232	The African Humid Period, rapid climate change events, the timing of human colonization, and megafaunal extinctions in Madagascar during the Holocene: Evidence from a 2m Anjohibe Cave stalagmite. Quaternary Science Reviews, 2019, 210, 136-153.	1.4	42
233	Testing the annual nature of speleothem banding. Scientific Reports, 2013, 3, 2633.	1.6	41
234	Lead concentrations and isotope ratios in speleothems as proxies for atmospheric metal pollution since the industrial revolution. Chemical Geology, 2015, 401, 140-150.	1.4	41

#	Article	IF	CITATIONS
235	Shallow particulate organic carbon regeneration in the South Pacific Ocean. Proceedings of the National Academy of Sciences of the United States of America, 2019, 116, 9753-9758.	3.3	41
236	Paleoclimate implications of mass spectrometric dating of a British flowstone. Geology, 1995, 23, 309.	2.0	40
237	Radiocarbon Calibration/Comparison Records Based on Marine Sediments from the Pakistan and Iberian Margins. Radiocarbon, 2013, 55, 1999-2019.	0.8	40
238	An extended and higher-resolution record of climate and land use from stalagmite MCO1 from Macal Chasm, Belize, revealing connections between major dry events, overall climate variability, and Maya sociopolitical changes. Palaeogeography, Palaeoclimatology, Palaeoecology, 2016, 459, 268-288.	1.0	40
239	Archaic human remains from Hualongdong, China, and Middle Pleistocene human continuity and variation. Proceedings of the National Academy of Sciences of the United States of America, 2019, 116, 9820-9824.	3.3	40
240	Î' high-resolution late Holocene speleothem record from Kaite Cave, northern Spain: δ180 variability and possible causes. Quaternary International, 2008, 187, 40-51.	0.7	39
241	Flux of Particulate Elements in the North Atlantic Ocean Constrained by Multiple Radionuclides. Global Biogeochemical Cycles, 2018, 32, 1738-1758.	1.9	39
242	Gas Hydrate Dissociation During Sea‣evel Highstand Inferred From U/Th Dating of Seep Carbonate From the South China Sea. Geophysical Research Letters, 2019, 46, 13928-13938.	1.5	39
243	NALPS19: sub-orbital-scale climate variability recorded in northern Alpine speleothems during the last glacial period. Climate of the Past, 2020, 16, 29-50.	1.3	39
244	Three thousand years of extreme rainfall events recorded in stalagmites from Spring Valley Caverns, Minnesota. Earth and Planetary Science Letters, 2010, 300, 46-54.	1.8	38
245	Spatio-temporal evolution of Australasian monsoon hydroclimate over the last 40,000 years. Earth and Planetary Science Letters, 2019, 513, 103-112.	1.8	38
246	Constraints on deep water age and particle flux in the equatorial and South Atlantic Ocean based on seawater231Pa and230Th data. Geophysical Research Letters, 2001, 28, 3437-3440.	1.5	37
247	Holocene variability of East Asian summer monsoon as viewed from the speleothem <mmi:math xmlns:mml="http://www.w3.org/1998/Math/MathML" altimg="si1.svg"><mml:mi>i^</mml:mi><mml:msup><mml:mrow /><mml:mrow><mml:mn>18</mml:mn></mml:mrow></mml:mrow </mml:msup>O records in central</mmi:math 	1.8	37
248	A Chinese cave links climate change, social impacts and human adaptation over the last 500 years. Scientific Reports, 2015, 5, 12284.	1.6	36
249	Strong coupling of centennial-scale changes of Asian monsoon and soil processes derived from stalagmite l´ ¹⁸ O and l´ ¹³ C records, southern China. Quaternary Research, 2016, 85, 333-346.	1.0	36
250	Timing and duration of the East Asian summer monsoon maximum during the Holocene based on stalagmite data from North China. Holocene, 2018, 28, 1631-1641.	0.9	36
251	231Pa and 230Th in surface sediments of the Arctic Ocean: Implications for 231Pa/230Th fractionation, boundary scavenging, and advective export. Earth and Planetary Science Letters, 2005, 234, 235-248.	1.8	35
252	Vegetation and environmental changes in tropical South America from the last glacial to the Holocene documented by multiple cave sediment proxies. Earth and Planetary Science Letters, 2019, 524, 115717.	1.8	35

#	Article	IF	CITATIONS
253	Evidence for 800years of North Atlantic multi-decadal variability from a Puerto Rican speleothem. Earth and Planetary Science Letters, 2011, 308, 23-28.	1.8	34
254	The control of the tropical North Atlantic on Holocene millennial climate oscillations. Geology, 2017, 45, 303-306.	2.0	33
255	Precipitation changes over the eastern Bolivian Andes inferred from speleothem (δ18O) records for the last 1400 years. Earth and Planetary Science Letters, 2018, 494, 124-134.	1.8	33
256	A multimillennial climatic context for the megafaunal extinctions in Madagascar and Mascarene Islands. Science Advances, 2020, 6, .	4.7	33
257	Inter-relationship and environmental significance of stalagmite l´13C and l´18O records from Zhenzhu Cave, north China, over the last 130 ka. Earth and Planetary Science Letters, 2020, 536, 116149.	1.8	33
258	Solar forcing of Holocene droughts in a stalagmite record from West Virginia in eastâ€eentral North America. Geophysical Research Letters, 2008, 35, .	1.5	32
259	Replacement Times of a Spectrum of Elements in the North Atlantic Based on Thorium Supply. Global Biogeochemical Cycles, 2018, 32, 1294-1311.	1.9	32
260	High precision glacial–interglacial benthic foraminiferal Sr/Ca records from the eastern equatorial Atlantic Ocean and Caribbean Sea. Earth and Planetary Science Letters, 2001, 190, 197-209.	1.8	31
261	230Th and 231Pa in the Arctic Ocean: implications for particle fluxes and basin-scale Th/Pa fractionation. Earth and Planetary Science Letters, 2004, 227, 155-167.	1.8	31
262	Climate significance of speleothem δ18O from central China on decadal timescale. Journal of Asian Earth Sciences, 2015, 106, 150-155.	1.0	31
263	How Far North Did the African Monsoon Fringe Expand During the African Humid Period? Insights From Southwest Moroccan Speleothems. Geophysical Research Letters, 2019, 46, 14093-14102.	1.5	31
264	Reconstructing the western boundary variability of the Western Pacific Subtropical High over the past 200Âyears via Chinese cave oxygen isotope records. Climate Dynamics, 2019, 52, 3741-3757.	1.7	31
265	A novel application of triple oxygen isotope ratios of speleothems. Geochimica Et Cosmochimica Acta, 2020, 270, 360-378. Comment on "Radiocarbon calibration curve spanning 0 to 50,000 years BP based on paired	1.6	31
0.4.4	230Th/234U/238U and 14C dates on pristine corals―by R.G. Fairbanks et al. (Quaternary Science Reviews) Tj E	•	0
266	radiocarbon calibration beyond 26,000 years before present using fossil corals―by TC. Chiu et al. (Quaternary Science Reviews 24 (2005) 1797–1808)â~†â~†â~†â~†â~†doi of original article: 10.1016/j.quascirev.20	1.4 05.04.002	30 2.
267	Quaternary Science Reviews, 2006, 25, 855-862. Holocene and Eemian climatic optima in the Korean Peninsula based on textural and carbon isotopic records from the stalagmite of the Daeya Cave, South Korea. Quaternary Science Reviews, 2011, 30, 1218-1231.	1.4	30
268	Coral record of reduced El Nino activity in the early 15th to middle 17th centuries. Geology, 2013, 41, 51-54.	2.0	30
269	Upper Pleistocene and Holocene palaeoenvironmental records in Cueva Mayor karst (Atapuerca, Spain) from different proxies: speleothem crystal fabrics, palynology, and archaeology. International Journal of Speleology, 2014, 43, 1-14.	0.4	30
270	Changing amounts and sources of moisture in the U.S. southwest since the Last Glacial Maximum in response to global climate change. Earth and Planetary Science Letters, 2014, 401, 47-56.	1.8	30

#	Article	IF	CITATIONS
271	Complicated responses of stalagmite δ13C to climate change during the last glaciation from Hulu Cave, Nanjing, China. Science in China Series D: Earth Sciences, 2005, 48, 2174-2181.	0.9	29
272	Mass spectrometric U-series dating of Laibin hominid site in Guangxi, southern China. Journal of Archaeological Science, 2007, 34, 2109-2114.	1.2	29
273	Milankovitch-paced Termination II in a Nevada speleothem?. Geophysical Research Letters, 2011, 38, n/a-n/a.	1.5	29
274	Freshwater tufa record from Spain supports evidence for the past interglacial being wetter than the Holocene in the Mediterranean region. Global and Planetary Change, 2011, 77, 129-141.	1.6	29
275	Potential influence of temperature changes in the Southern Hemisphere on the evolution of the Asian summer monsoon during the last glacial period. Quaternary International, 2016, 392, 239-250.	0.7	29
276	Multi-decadal to centennial hydro-climate variability and linkage to solar forcing in the Western Mediterranean during the last 1000 years. Scientific Reports, 2018, 8, 17446.	1.6	29
277	Initiation of a stable convective hydroclimatic regime in Central America circa 9000 years BP. Nature Communications, 2020, 11, 716.	5.8	29
278	Uranium-Series Dating of Speleothems: Current Techniques, Limits, & Applications. , 2004, , 177-197.		29
279	Mass spectrometric dating of flowstones from Stump Cross Caverns and Lancaster Hole, Yorkshire: palaeoclimate implications. , 1996, 11, 107-114.		28
280	Large variations of <scp>l´^{l3}C</scp> values in stalagmites from southeastern <scp>C</scp> hina during historical times: implications for anthropogenic deforestation. Boreas, 2015, 44, 511-525.	1.2	28
281	Onset and duration of transitions into Greenland Interstadials 15.2 and 14 in northern China constrained by an annually laminated stalagmite. Scientific Reports, 2016, 6, 20844.	1.6	28
282	New speleothem data from Molinos and Ejulve caves reveal Holocene hydrological variability in northeast Iberia. Quaternary Research, 2017, 88, 223-233.	1.0	28
283	The Hekla 3 volcanic eruption recorded in a Scottish speleothem?. Holocene, 1995, 5, 336-342.	0.9	27
284	A stalagmite record of abrupt climate change and possible Westerlies-derived atmospheric precipitation during the Penultimate Glacial Maximum in northern China. Palaeogeography, Palaeoclimatology, Palaeoecology, 2014, 393, 30-44.	1.0	27
285	A 3000-yr Annually Laminated Stalagmite Record of the Last Glacial Maximum from Hulu Cave, China. Quaternary Research, 2015, 83, 360-369.	1.0	27
286	A high-resolution fluid inclusion δ18O record from a stalagmite in SW France: modern calibration and comparison with multiple proxies. Quaternary Science Reviews, 2015, 110, 152-165.	1.4	27
287	Paleoclimate in continental northwestern Europe during the Eemian and early Weichselian (125–97â€⁻ka): insights from a Belgian speleothem. Climate of the Past, 2016, 12, 1445-1458.	1.3	27
288	Calibration of speleothem δ 18 O records against hydroclimate instrumental records in Central Brazil. Global and Planetary Change, 2016, 139, 151-164.	1.6	27

#	Article	IF	CITATIONS
289	Great flood in the middle-lower Yellow River reaches at 4000 a BP inferred from accurately-dated stalagmite records. Science Bulletin, 2018, 63, 206-208.	4.3	27
290	Alpine permafrost thawing during the Medieval Warm Period identified from cryogenic cave carbonates. Cryosphere, 2013, 7, 1073-1081.	1.5	26
291	Long-term changes in precipitation recorded by magnetic minerals in speleothems. Geology, 2015, 43, 595-598.	2.0	26
292	Interpretation of orbital scale variability in mid-latitude speleothem δ18O: Significance of growth rate controlled kinetic fractionation effects. Quaternary Science Reviews, 2015, 127, 215-228.	1.4	26
293	Natural attrition and growth frequency variations of stalagmites in southwest Sulawesi over the past 530,000 years. Palaeogeography, Palaeoclimatology, Palaeoecology, 2016, 441, 823-833.	1.0	26
294	Stalagmite-inferred centennial variability of the Asian summer monsoon in southwest China between 58 and 79Âka BP. Quaternary Science Reviews, 2017, 160, 1-12.	1.4	26
295	Geochemistry of speleothems affected by aragonite to calcite recrystallization – Potential inheritance from the precursor mineral. Geochimica Et Cosmochimica Acta, 2017, 200, 310-329.	1.6	26
296	Abrupt climate changes during Termination III in Southern Europe. Proceedings of the National Academy of Sciences of the United States of America, 2017, 114, 10047-10052.	3.3	26
297	Climate changes in Northeastern Brazil from deglacial to Meghalayan periods and related environmental impacts. Quaternary Science Reviews, 2020, 250, 106655.	1.4	26
298	Variation in the Asian monsoon intensity and dry–wet conditions since the Little Ice Age in central China revealed by an aragonite stalagmite. Climate of the Past, 2014, 10, 1803-1816.	1.3	25
299	Timing and nature of the penultimate deglaciation in a high alpine stalagmite from Switzerland. Quaternary Science Reviews, 2015, 126, 264-275.	1.4	25
300	Evidence of thermophilisation and elevation-dependent warming during the Last Interglacial in the Italian Alps. Scientific Reports, 2018, 8, 2680.	1.6	25
301	Geochronology, sediment provenance, and fossil emplacement at Sumidouro Cave, a classic late Pleistocene/early Holocene Paleoanthropological site in eastern Brazil. Geoarchaeology - an International Journal, 2005, 20, 751-764.	0.7	24
302	A method to anchor floating chronologies in annually laminated speleothems with U–Th dates. Quaternary Geochronology, 2012, 14, 57-66.	0.6	24
303	Contrasting Patterns in Abrupt Asian Summer Monsoon Changes in the Last Glacial Period and the Holocene. Paleoceanography and Paleoclimatology, 2018, 33, 214-226.	1.3	24
304	Speleothem record of geomagnetic South Atlantic Anomaly recurrence. Proceedings of the National Academy of Sciences of the United States of America, 2018, 115, 13198-13203.	3.3	24
305	Dating of the Devils Hole Calcite Vein. Science, 1993, 259, 1626-1626.	6.0	23
306	A dry episode during the Younger Dryas and centennialâ€scale weak monsoon events during the early Holocene: A highâ€resolution stalagmite record from southeast of the Loess Plateau, China. Geophysical Research Letters, 2008, 35, .	1.5	23

#	Article	IF	CITATIONS
307	Data reporting standards for publication of U-series data for geochronology and timescale assessment in the earth sciences. Quaternary Geochronology, 2017, 39, 142-149.	0.6	23
308	Three distinct Holocene intervals of stalagmite deposition and nondeposition revealed in NW Madagascar, and their paleoclimate implications. Climate of the Past, 2017, 13, 1771-1790.	1.3	23
309	Is Chinese stalagmite δ18O solely controlled by the Indian summer monsoon?. Climate Dynamics, 2019, 53, 2969-2983.	1.7	23
310	Radiocarbon Results from a 13-Kyr BP Coral from the Huon Peninsula, Papua New Guinea. Radiocarbon, 2004, 46, 1211-1224.	0.8	22
311	U-series disequilibria in Guatemalan lavas, crustal contamination, and implications for magma genesis along the Central American subduction zone. Journal of Geophysical Research, 2007, 112, .	3.3	22
312	Igneous Origin of CO2 in Ancient and Recent Hot-Spring Waters and Travertines from the Northern Argentinean Andes. Journal of Sedimentary Research, 2009, 79, 554-567.	0.8	22
313	Estimating the upper limit of prehistoric peak ground acceleration using an in situ, intact and vulnerable stalagmite from PlaveckĄ̃; priepast cave (DetrekÅʻi-zsomboly), Little Carpathians, Slovakia—first results. Journal of Seismology, 2017, 21, 1111-1130.	0.6	22
314	Stalagmite multi-proxy evidence of wet and dry intervals in northeastern Namibia: Linkage to latitudinal shifts of the Inter-Tropical Convergence Zone and changing solar activity from AD 1400 to 1950. Holocene, 2017, 27, 384-396.	0.9	22
315	Reconstruction of Holocene coupling between the South American Monsoon System and local moisture variability from speleothem Î'180 and 87Sr/86Sr records. Quaternary Science Reviews, 2019, 210, 51-63.	1.4	22
316	Investigating the 8.2 ka event in northwestern Madagascar: Insight from data–model comparisons. Quaternary Science Reviews, 2019, 204, 172-186.	1.4	22
317	Mass spectrometric U-series dating of New Cave at Zhoukoudian, China. Journal of Archaeological Science, 2004, 31, 337-342.	1.2	21
318	Multiproxy evidence from caves of Native Americans altering the overlying landscape during the late Holocene of east-central North America. Holocene, 2010, 20, 275-283.	0.9	21
319	Great Basin hydrology, paleoclimate, and connections with the North Atlantic: A speleothem stable isotope and trace element record from Lehman Caves, NV. Quaternary Science Reviews, 2015, 127, 186-198.	1.4	21
320	Multi-scale Holocene Asian monsoon variability deduced from a twin-stalagmite record in southwestern China. Quaternary Research, 2016, 86, 34-44.	1.0	21
321	Exceptional warmth and climate instability occurred in the European Alps during the Last Interglacial period. Communications Earth & Environment, 2020, 1, .	2.6	21
322	Penultimate deglaciation Asian monsoon response to North Atlantic circulation collapse. Nature Geoscience, 2021, 14, 937-941.	5.4	21
323	Age and significance of the Quaternary cemented deposits of the Duje Valley (Picos de Europa,) Tj ETQq1 1 0.78	4314 rgBT 1.0	Qverlock 10
394	Cyclic changes of Asian monsoon intensity during the early mid-Holocene from annually-laminated	14	20

stalagmites, central China. Quaternary Science Reviews, 2015, 121, 1-10.

1.4 20

#	Article	IF	CITATIONS
325	East Asian monsoon changes early in the last deglaciation and insights into the interpretation of oxygen isotope changes in the Chinese stalagmite record. Quaternary Science Reviews, 2020, 250, 106699.	1.4	20
326	A severe drought during the last millennium in East Java, Indonesia. Quaternary Science Reviews, 2013, 80, 102-111.	1.4	19
327	Testing models of thorium and particle cycling in the ocean using data from station GT11-22 of the U.S. GEOTRACES North Atlantic section. Deep-Sea Research Part I: Oceanographic Research Papers, 2016, 113, 57-79.	0.6	19
328	Three-phased Heinrich Stadial 4 recorded in NE Brazil stalagmites. Earth and Planetary Science Letters, 2019, 510, 94-102.	1.8	19
329	Human activity and climate change triggered the expansion of rocky desertification in the karst areas of Southwestern China. Science China Earth Sciences, 2021, 64, 1761-1773.	2.3	19
330	The Y. D. and climate abrupt events in the early and middle Holocene: Stalagmite oxygen isotope record from Maolan, Guizhou, China. Science in China Series D: Earth Sciences, 2005, 48, 530-537.	0.9	18
331	Holocene flood frequency reconstruction from speleothems inÂnorthern Spain. Quaternary Science Reviews, 2015, 127, 129-140.	1.4	18
332	A multi-proxy stalagmite record from northwestern Namibia of regional drying with increasing global-scale warmth over the last 47 kyr: The interplay of a globally shifting ITCZ with regional currents, winds, and rainfall. Palaeogeography, Palaeoclimatology, Palaeoecology, 2016, 461, 109-121.	1.0	18
333	Quaternary depositional facies in cave entrances and their relation to landscape evolution: The example of Cuvieri Cave, eastern Brazil. Catena, 2017, 157, 372-387.	2.2	18
334	Hydro-climatic variability in the southwestern Indian Ocean between 6000 and 3000 years ago. Climate of the Past, 2018, 14, 1881-1891.	1.3	18
335	Moisture availability in the southwest United States over the last three glacial-interglacial cycles. Science Advances, 2018, 4, eaau1375.	4.7	18
336	Late Holocene monsoon precipitation changes in southern China and their linkage to Northern Hemisphere temperature. Quaternary Science Reviews, 2020, 232, 106191.	1.4	18
337	Droughts and societal change: The environmental context for the emergence of Islam in late Antique Arabia. Science, 2022, 376, 1317-1321.	6.0	18
338	An ancient shallow slip event on the Mentawai segment of the Sunda megathrust, Sumatra. Journal of Geophysical Research, 2012, 117, .	3.3	17
339	The 7.2 ka climate event: Evidence from high-resolution stable isotopes and trace element records of stalagmite in Shuiming Cave, Chongqing, China. Holocene, 2020, 30, 145-154.	0.9	17
340	Relationships between climate change, human environmental impact, and megafaunal extinction inferred from a 4000-year multi-proxy record from a stalagmite from northwestern Madagascar. Quaternary Science Reviews, 2020, 234, 106244.	1.4	17
341	Comment on "On linking climate to Chinese dynastic change: Spatial and temporal variations of monsoonal rain― Science Bulletin, 2010, 55, 3734-3737.	1.7	16
342	A record of wet glacial stages and dry interglacial stages over the last 560 kyr from a standing massive stalagmite in Carlsbad Cavern, New Mexico, USA. Palaeogeography, Palaeoclimatology, Palaeoecology, 2015, 438, 256-266.	1.0	16

#	Article	IF	CITATIONS
343	A comparison of <scp>U</scp> / <scp>T</scp> h and rapidâ€screen ¹⁴ <scp>C</scp> dates from <scp>L</scp> ine <scp>I</scp> sland fossil corals. Geochemistry, Geophysics, Geosystems, 2016, 17, 833-845.	1.0	16
344	Evolution of the Asian summer monsoon during Dansgaard/Oeschger events 13–17 recorded in a stalagmite constrained by high-precision chronology from southwest China. Quaternary Research, 2017, 88, 121-128.	1.0	16
345	Orbital-to-millennial scale climate variability during Marine Isotope Stages 5 to 3 in northeast Iberia. Quaternary Science Reviews, 2019, 224, 105946.	1.4	16
346	Paleotopography of Glacial-Age Ice Sheets. Science, 1995, 267, 536-536.	6.0	15
347	Variable rates of Late Quaternary surface uplift along the Banda Arc-Australian plate collision zone, eastern Indonesia. Geological Society Special Publication, 1999, 146, 213-224.	0.8	15
348	Sr/Ca-Sea surface temperature calibration in the branching Caribbean coralAcropora palmata. Geophysical Research Letters, 2006, 33, .	1.5	15
349	Long-term hydrological changes in northern Iberia (4.9–0.9 ky BP) from speleothem Mg/Ca ratios and cave monitoring (Ojo GuareA±a Karst Complex, Spain). Environmental Earth Sciences, 2015, 74, 7741-7753.	1.3	15
350	Millennial and orbital scale variability of the South American Monsoon during the penultimate glacial period. Scientific Reports, 2019, 9, 1234.	1.6	15
351	A multiple-proxy stalagmite record reveals historical deforestation in central Shandong, northern China. Science China Earth Sciences, 2020, 63, 1622-1632.	2.3	15
352	Strong links between Saharan dust fluxes, monsoon strength, and North Atlantic climate during the last 5000 years. Science Advances, 2021, 7, .	4.7	15
353	Heterogenous Late Holocene Climate in the Eastern Mediterranean—The Kocain Cave Record From SW Turkey. Geophysical Research Letters, 2021, 48, e2021GL094733.	1.5	15
354	Holocene variability in the intensity of wind-gap upwelling in the tropical eastern Pacific. Paleoceanography, 2015, 30, 1113-1131.	3.0	14
355	Millennial-scale variability in the local radiocarbon reservoir age of south Florida during the Holocene. Quaternary Geochronology, 2017, 42, 130-143.	0.6	14
356	Ion microprobe δ18O analyses to calibrate slow growth rate speleothem records with regional δ18O records of precipitation. Earth and Planetary Science Letters, 2018, 482, 367-376.	1.8	14
357	Importance of Hydrothermal Vents in Scavenging Removal of ²³⁰ Th in the Nansen Basin. Geophysical Research Letters, 2018, 45, 10,539.	1.5	14
358	A new speleothem record of the penultimate deglacial: Insights into spatial variability and centennial-scale instabilities of East Asian monsoon. Quaternary Science Reviews, 2019, 210, 113-124.	1.4	14
359	From cave geomorphology to Palaeolithic human behaviour: speleogenesis, palaeoenvironmental changes and archaeological insight in the Atxurraâ€Armiña cave (northern Iberian Peninsula). Journal of Quaternary Science, 2020, 35, 841-853.	1.1	14
360	Karst hydrological changes during the Late-Holocene in Southwestern China. Quaternary Science Reviews, 2021, 258, 106865.	1.4	14

#	Article	IF	CITATIONS
361	Onset and termination of Heinrich Stadial 4 and the underlying climate dynamics. Communications Earth & Environment, 2021, 2, .	2.6	14
362	Radiometric, isotopic, and petrographic evidence of changing interglacials over the past 550,000 years from six stalagmites from the Serra do Courel in the Cordillera Cantábrica of northwestern Spain. Palaeogeography, Palaeoclimatology, Palaeoecology, 2017, 466, 137-152.	1.0	13
363	Climate dynamics during the penultimate glacial period recorded in a speleothem from Kanaan Cave, Lebanon (central Levant). Quaternary Research, 2018, 90, 10-25.	1.0	13
364	Eastern North American climate in phase with fall insolation throughout the last three glacial-interglacial cycles. Earth and Planetary Science Letters, 2019, 522, 125-134.	1.8	13
365	Ocean-atmosphere interconnections from the last interglacial to the early glacial: An integration of marine and cave records in the Iberian region. Quaternary Science Reviews, 2019, 226, 106037.	1.4	13
366	Medieval Climate Variability in the eastern Amazon-Cerrado regions and its archeological implications. Scientific Reports, 2019, 9, 20306.	1.6	13
367	Changes in Circulation and Particle Scavenging in the Amerasian Basin of the Arctic Ocean over the Last Three Decades Inferred from the Water Column Distribution of Geochemical Tracers. Journal of Geophysical Research: Oceans, 2019, 124, 9338-9363.	1.0	13
368	High precise dating on the variation of the Asian summer monsoon since 37Âka BP. Scientific Reports, 2021, 11, 9375.	1.6	13
369	Rapid northern hemisphere ice sheet melting during the penultimate deglaciation. Nature Communications, 2022, 13, .	5.8	13
370	Time scale of magma differentiation in arcs from protactinium-radium isotopic data. Geology, 2005, 33, 633-636.	2.0	12
371	Correction to "A dry episode during the Younger Dryas and centennialâ€scale weak monsoon events during the early Holocene: A highâ€resolution stalagmite record from southeast of the Loess Plateau, Chinaâ€r Geophysical Research Letters, 2008, 35, .	1.5	12
372	Composition and sources of lipid compounds in speleothem calcite from southwestern Oregon and their paleoenvironmental implications. Environmental Earth Sciences, 2011, 62, 1245-1261.	1.3	12
373	A 500-year seasonally resolved Î ¹⁸ O and Î ¹³ C, layer thickness and calcite aspect record from a speleothem deposited in the Han-sur-Lesse cave, Belgium. Climate of the Past, 2015, 11, 789-802.	1.3	12
374	Highâ€resolution reconstruction of 8.2â€ka BP event documented in Père Noël cave, southern Belgium. Journal of Quaternary Science, 2018, 33, 840-852.	1.1	12
375	Distinct Permafrost Conditions Across the Last Two Glacial Periods in Midlatitude North America. Geophysical Research Letters, 2019, 46, 13318-13326.	1.5	12
376	A Highâ€Resolution Speleothem Record of Marine Isotope Stage 11 as a Natural Analog to Holocene Asian Summer Monsoon Variations. Geophysical Research Letters, 2019, 46, 9949-9957.	1.5	12
377	Timescales of hydrothermal scavenging in the South Pacific Ocean from 234Th, 230Th, and 228Th. Earth and Planetary Science Letters, 2019, 506, 146-156.	1.8	12
378	A Continuous Record of Central Tropical Pacific Climate Since the Midnineteenth Century Reconstructed From Fanning and Palmyra Island Corals: A Case Study in Coral Data Reanalysis. Paleoceanography and Paleoclimatology, 2020, 35, e2020PA003848.	1.3	12

#	Article	IF	CITATIONS
379	Little Ice Age climate changes in Southwest China from a stalagmite δ180 record. Palaeogeography, Palaeoclimatology, Palaeoecology, 2021, 562, 110167.	1.0	12
380	Impacts of Coral Growth on Geochemistry: Lessons From the Galápagos Islands. Paleoceanography and Paleoclimatology, 2021, 36, e2020PA004051.	1.3	12
381	A multi-proxy climate record from a northwestern Botswana stalagmite suggesting wetness late in the Little Ice Age (1810–1820—CE) and drying thereafter in response to changing migration of the tropical rain belt or ITCZ. Palaeogeography, Palaeoclimatology, Palaeoecology, 2018, 506, 139-153.	1.0	11
382	Millennial-scale glacial climate variability in Southeastern Alaska follows Dansgaard-Oeschger cyclicity. Scientific Reports, 2019, 9, 7880.	1.6	11
383	Timing and structure of the weak Asian Monsoon event about 73,000 years ago. Quaternary Geochronology, 2019, 53, 101003.	0.6	11
384	A 120-year seasonally resolved speleothem record of precipitation seasonality from southeastern China. Quaternary Science Reviews, 2021, 264, 107023.	1.4	11
385	Hydroclimate variability during the last 2700 years based on stalagmite multi-proxy records in the central-western Mediterranean. Quaternary Science Reviews, 2021, 269, 107137.	1.4	11
386	Environmental influences on speleothem growth in southwestern Oregon during the last 380000Âyears. Earth and Planetary Science Letters, 2009, 279, 316-325.	1.8	10
387	Textural and carbon isotopic evidence of monsoonal changes recorded in a composite-type speleothem from Korea since MIS 5a. Quaternary Research, 2010, 74, 100-112.	1.0	10
388	East central North America climates during marine isotope stages 3-5. Geophysical Research Letters, 2014, 41, 3233-3237.	1.5	10
389	Upper Pleistocene interstratal piping-cave speleogenesis: The Seso Cave System (Central Pyrenees,) Tj ETQq1 1	0.784314 1.1	Frg₽Ţ/Overl⊃c
390	Multi-scale Holocene Asian monsoon variability deduced from a twin-stalagmite record in southwestern China. Quaternary Research, 2016, 86, 34-44.	1.0	10
391	Timing and structure of Termination II in north China constrained by a precisely dated stalagmite record. Earth and Planetary Science Letters, 2019, 512, 1-7.	1.8	10
392	Holocene and deglaciation hydroclimate changes in northern China as inferred from stalagmite growth frequency. Global and Planetary Change, 2020, 195, 103360.	1.6	10
393	U-Th dating of lake sediments: Lessons from the 700 ka sediment record of Lake JunÃn, Peru. Quaternary Science Reviews, 2020, 244, 106422.	1.4	10
394	Millennial-scale Asian monsoon variability during MIS 9 revealed by a high-resolution stalagmite δ18O record in Luoshui Cave, central China. Quaternary Science Reviews, 2020, 234, 106218.	1.4	10
395	Changing chemistry of particulate manganese in the near- and far-field hydrothermal plumes from 15ŰS East Pacific Rise and its influence on metal scavenging. Geochimica Et Cosmochimica Acta, 2021, 300, 95-118.	1.6	10
396	Precise timing of MIS 7 substages from the Austrian Alps. Climate of the Past, 2021, 17, 1443-1454.	1.3	10

#	Article	IF	CITATIONS
397	Time scale of magma differentiation in arcs from protactinium-radium isotopic data. Geology, 2005, 33, 633.	2.0	10
398	Modulation of centennial-scale hydroclimate variations in the middle Yangtze River Valley by the East Asian-Pacific pattern and ENSO over the past two millennia. Earth and Planetary Science Letters, 2021, 576, 117220.	1.8	10
399	A high-resolution stalagmite record from Luoshui Cave, Central China over the past 23.5 kyr. Quaternary Science Reviews, 2022, 282, 107443.	1.4	10
400	A possible Younger Dryas-type event during Asian monsoonal Termination 3. Science in China Series D: Earth Sciences, 2006, 49, 982-990.	0.9	9
401	Millennial-scale interhemispheric asymmetry of low-latitude precipitation: Speleothem evidence and possible high-latitude forcing. Geophysical Monograph Series, 2007, , 279-294.	0.1	9
402	Reconstruction of the Northeast Asian monsoon climate history for the past 400 years based on textural, carbon and oxygen isotope record of a stalagmite from Yongcheon lava tube cave, Jeju Island, Korea. Quaternary International, 2015, 384, 37-51.	0.7	9
403	Last glacial and Holocene stable isotope record of fossil dripwater from subtropical Brazil based on analysis of fluid inclusions in stalagmites. Chemical Geology, 2017, 468, 84-96.	1.4	9
404	Application of Avaatech X-ray fluorescence core-scanning in Sr/Ca analysis of speleothems. Science China Earth Sciences, 2019, 62, 964-973.	2.3	9
405	Characterizing the Eemian-Weichselian transition in northwestern Europe with three multiproxy speleothem archives from the Belgian Han-sur-Lesse and Remouchamps cave systems. Quaternary Science Reviews, 2019, 208, 21-37.	1.4	9
406	Black carbon traces of human activities in stalagmites from Turkey. Journal of Archaeological Science, 2020, 123, 105255.	1.2	9
407	A Last Interglacial speleothem record from the Sieben Hengste cave system (Switzerland): Implications for alpine paleovegetation. Quaternary Science Reviews, 2021, 262, 106974.	1.4	9
408	Integrating U-Th, ¹⁴ C, and ²¹⁰ Pb methods to produce a chronologically reliable isotope record for the Belize River Valley Maya from a low-uranium stalagmite. Holocene, 2019, 29, 1234-1248.	0.9	8
409	Centennial-scale climatic changes in Central China during the Holocene climatic optimum. Palaeogeography, Palaeoclimatology, Palaeoecology, 2020, 558, 109950.	1.0	8
410	Paleohydrology of southwest Nevada (USA) based on groundwater 234U/238U over the past 475 k.y Bulletin of the Geological Society of America, 2020, 132, 793-802.	1.6	8
411	Speleothem record of mild and wet mid-Pleistocene climate in northeast Greenland. Science Advances, 2021, 7, .	4.7	8
412	Uranium–Thorium Dating of Speleothems. Elements, 2021, 17, 87-92.	0.5	8
413	Timing and structure of early-Holocene climate anomalies inferred from north Chinese stalagmite records. Holocene, 2021, 31, 1777-1785.	0.9	8
414	Seasonality of precipitation recorded in a modern (1907–2008) annually laminated stalagmite from central China. Palaeogeography, Palaeoclimatology, Palaeoecology, 2021, 576, 110489.	1.0	8

#	Article	IF	CITATIONS
415	Oldest Dryas hydroclimate reorganization in the eastern Iberian Peninsula after the iceberg discharges of Heinrich Event 1. Quaternary Research, 2021, 101, 67-83.	1.0	8
416	Uranium-Series Dating Of Speleothemes: Current Techniques, Limits amp; Applications. , 2007, , 177-197.		8
417	Highly resolved δ13C and trace element ratios of precisely dated stalagmite from northwestern China: Hydroclimate reconstruction during the last two millennia. Quaternary Science Reviews, 2022, 291, 107473.	1.4	8
418	Evidence of Holocene uplift in east New Britain, Papua New Guinea. Geophysical Research Letters, 2006, 33, n/a-n/a.	1.5	7
419	Carbon and oxygen isotope records and paleoclimate reconstruction (140–250Âka B.P.) from a stalagmite of Shuinan Cave, Guilin, China. Environmental Geology, 2006, 49, 752-764.	1.2	7
420	East Asian summer monsoon climates and cave hydrological cycles over Dansgaard-Oeschger events 14 to 11 revealed by a new stalagmite record from Hulu Cave. Quaternary Research, 2019, 92, 725-737.	1.0	7
421	U-Th and radiocarbon dating of calcite speleothems from gypsum caves (Emilia Romagna, North Italy). Quaternary Geochronology, 2019, 52, 51-62.	0.6	7
422	Paleovegetation seesaw in Brazil since the Late Pleistocene: A multiproxy study of two biomes. Earth and Planetary Science Letters, 2021, 563, 116880.	1.8	7
423	Early Holocene permafrost retreat in West Siberia amplified by reorganization of westerly wind systems. Communications Earth & Environment, 2021, 2, .	2.6	7
424	Last interglacial hydroclimate in the Italian Prealps reconstructed from speleothem multi-proxy records (Bigonda Cave, NE Italy). Quaternary Science Reviews, 2021, 272, 107243.	1.4	7
425	Additional multi-proxy stalagmite evidence from northeast Namibia supports recent models of wetter conditions during the 4.2Åka Event in the Southern Hemisphere. Palaeogeography, Palaeoclimatology, Palaeoecology, 2022, 586, 110756.	1.0	7
426	Different response of stalagmite δ18O and δ13C to millennial-scale events during the last glacial, evidenced from Huangjin Cave, northern China. Quaternary Science Reviews, 2022, 276, 107305.	1.4	7
427	Indian summer monsoon variations during the Younger Dryas as revealed by a laminated stalagmite record from the Tibetan Plateau. Quaternary Science Reviews, 2022, 278, 107375.	1.4	7
428	Paleoclimatic and paleoenvironmental changes in Amazonian lowlands over the last three millennia. Quaternary Science Reviews, 2022, 279, 107383.	1.4	7
429	Geomorphology and genesis of the remarkable Araras Ridge tufa deposit, Western Brazil. Geomorphology, 2011, 134, 94-101.	1.1	6
430	High-resolution stalagmite δ 13C record of soil processes from southwestern China during the early MIS 3. Science Bulletin, 2013, 58, 796-802.	1.7	6
431	Distribution Characteristics and Influencing Factors of Uranium Isotopes in Saline Lake Waters in the Northeast of Qaidam Basin. Minerals (Basel, Switzerland), 2020, 10, 74.	0.8	6
432	Gradual Southâ€North Climate Transition in the Atlantic Realm Within the Younger Dryas. Geophysical Research Letters, 2021, 48, e2021GL092620.	1.5	6

#	Article	IF	CITATIONS
433	Speleothemâ€Based Hydroclimate Reconstructions During the Penultimate Deglaciation in Northern China. Paleoceanography and Paleoclimatology, 2021, 36, e2020PA004072.	1.3	6
434	A NEW RECORD OF THE LATE PLEISTOCENE CORAL <i>POCILLOPORA PALMATA</i> FROM THE DRY TORTUGAS, FLORIDA REEF TRACT, USA. Palaios, 2015, 30, 827-835.	0.6	5
435	A tropical speleothem record of glacial inception, the South American Summer Monsoon from 125 to 115 ka. Climate of the Past, 2015, 11, 931-938.	1.3	5
436	Centennial-scale monsoon climate fluctuations from a stalagmite record during the mid-Holocene Epoch in Fulu cave of Huaping, Yunnan, China. Environmental Earth Sciences, 2015, 74, 929-935.	1.3	5
437	Glacial and interglacials in the Neotropics: a 130,000-year diatom record from central Panama. Journal of Paleolimnology, 2017, 58, 497-510.	0.8	5
438	7700-year persistence of an isolated, free-living coral assemblage in the Galápagos Islands: a model for coral refugia?. Coral Reefs, 2020, 39, 639-647.	0.9	5
439	Variability of PDO identified by a last 300-year stalagmite δ180 record in Southwest China. Quaternary Science Reviews, 2021, 261, 106947.	1.4	5
440	Marginal Reefs Under Stress: Physiological Limits Render Galápagos Corals Susceptible to Ocean Acidification and Thermal Stress. AGU Advances, 2022, 3, .	2.3	5
441	Control of insolation on stalagmite growth, rainfall, and migration of the tropical rain belt in northern Namibia over the last 100†kyr, as suggested by a rare MIS 5b-5c stalagmite from Dante Cave. Palaeogeography, Palaeoclimatology, Palaeoecology, 2019, 535, 109348.	1.0	4
442	Influences on Asian summer monsoon during Dansgaard-Oeschger events 19 to 25 (70–115 kyr B.P.). Palaeogeography, Palaeoclimatology, Palaeoecology, 2022, 587, 110798.	1.0	4
443	Stalagmite paleomagnetic record of a quiet mid-to-late Holocene field activity in central South America. Nature Communications, 2022, 13, 1349.	5.8	4
444	Early Last Interglacial environmental changes recorded by speleothems from Katerloch (southâ€east) Tj ETQq0 0	0 rgBT /Ov	verlock 10 Tf
445	Ice Age Rhythms. Science, 2010, 327, 790-791.	6.0	3
446	Remote vs. local control on the Preboreal Asian hydroclimate and soil processes recorded by an annually-laminated stalagmite from Daoguan Cave, southern China. Quaternary International, 2017, 452, 79-90.	0.7	3
447	Summer Monsoon Rainfall Variability in Central China over the Past 4700 Years and Its Possible Link to Solar Activity. Journal of Meteorological Research, 2021, 35, 594-606.	0.9	3
448	ldentification of a Quaternary rock avalanche deposit (Central Apennines, Italy): Significance for recognition of fossil catastrophic massâ€wasting. Sedimentology, 2022, 69, 2099-2130.	1.6	3
449	U/Th and U/Pa dating of nanjing man and peking man. Science Bulletin, 1998, 43, 26-26.	1.7	2
450	Corrigendum to "Quaternary glaciation and hydrologic variation in the South American tropics as reconstructed from the Lake Titicaca drilling project" [Quaternary Research 68 (2007) 410–420]. Quaternary Research, 2008, 69, 342-342.	1.0	2

#	Article	IF	CITATIONS
451	²³⁰ Th dating of flowstone from Ignatievskaya Cave, Russia: Age constraints of rock art and paleoclimate inferences. Geoarchaeology - an International Journal, 2021, 36, 532-545.	0.7	2
452	Novel method for determining ²³⁴ U– ²³⁸ U ages of Devils Hole 2 cave calcite (Nevada). Geochronology, 2021, 3, 49-58.	1.0	2
453	Trace Elements in Speleothems as Indicators of Past Climate and Karst Hydrochemistry: A Case Study from Kaite Cave (N Spain). , 2015, , 569-577.		2
454	17. Les variations de la mousson et la société chinoise depuis 1 800 ans. , 2012, , 291-306.		2
455	Effects of Ice Freeze-Thaw Processes on U Isotope Compositions in Saline Lakes and Their Potential Environmental Implications. Frontiers in Earth Science, 2021, 9, .	0.8	2
456	Central Equatorial Pacific Warming and Freshening in the Twentieth Century: Insights From a Coral Ensemble Approach. Geophysical Research Letters, 2022, 49, .	1.5	2
457	Application of cave monitoring to constrain the value and source of detrital 230Th/232Th in speleothem calcite: Implications for U-series geochronology of speleothems. Palaeogeography, Palaeoclimatology, Palaeoecology, 2022, 596, 110978.	1.0	2
458	Hydroclimatic changes in south-central China during the 4.2 ka event and their potential impacts on the development of Neolithic culture. Quaternary Research, 2022, 109, 39-52.	1.0	2
459	ENSO effect on hydroclimate changes in southeastern China over the past two millennia. Quaternary Science Reviews, 2022, 285, 107539.	1.4	2
460	Response to Comments on "Reconciliation of the Devils Hole climate record with orbital forcing― Science, 2016, 354, 296-296.	6.0	1
461	The "Hockey Stick―Imprint in Northwest African Speleothems. Geophysical Research Letters, 2021, 48, e2021GL094232.	1.5	1
462	First pre-modern record of the gyrfalcon (Falco rusticolus) in north-east Greenland. Polar Research, 2019, 38, .	1.6	1
463	Paleotopography of Glacial-Age Ice Sheets. Science, 1995, 267, 536-536.	6.0	1
464	Climatic and anthropogenic influence on vegetation in southeastern China during the past 120 years inferred from speleothem. Quaternary International, 2022, 625, 60-65.	0.7	1
465	Asian Summer Monsoon Changes Inferred From a Stalagmite δ180 Record in Central China During the Last Glacial Period. Frontiers in Earth Science, 2022, 10, .	0.8	1
466	Episodic deposition of stalagmites in the northeastern Democratic Republic of the Congo suggests Equatorial Humid Periods during insolation maxima. Quaternary Science Reviews, 2022, 286, 107552.	1.4	1
467	Glacial sea surface temperature reconstruction in the west pacific warm pool. Science Bulletin, 1998, 43, 89-89.	1.7	0
468	Acceptance of the 2008 Nicholas J. Shackleton Award. Geochimica Et Cosmochimica Acta, 2009, 73, S17.	1.6	0

#	ARTICLE	IF	CITATIONS
469	Reply to Comment by DomÃnguez-Villar on "Land surface temperature changes in Northern Iberia since 4000yr BP, based in δ13C of speleothems―(MartÃn-Chivelet et al., 2011). Global and Planetary Change, 2013, 101, 129-130.	1.6	Ο
470	Woo et al. reply. Nature, 2015, 526, E2-E3.	13.7	0
471	Response to Comment on "No consistent ENSO response to volcanic forcing over the last millennium― Science, 2020, 369, .	6.0	0